Supporting Information

RuO$_2$/NiRu Heterojunction Optimizes d-band Center of Ni−Ru Catalyst for High-Performance Alkaline Hydrogen Evolution Reaction

Yitian Zhou[1], Yifan Liu[1], Hehua Tang[1], and Bolin Lin*[1]

[1]School of Physical Science and Technology, ShanghaiTech University, Shanghai 201210, China.

*Corresponding authors' E-mails: linbl@shangaitech.edu.cn

This PDF file includes:
- Figure S1 to S14
- Table S1 to S7
- References
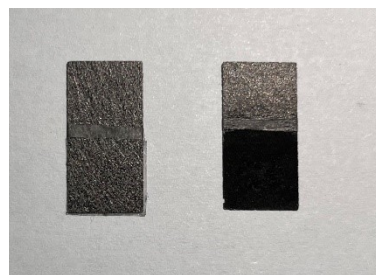
Figure S1. The photograph of blank carbon paper (left) and the electrode of Ni1Ru1/C

(right).

The milky white tape was to ensure the loading area of the catalyst.
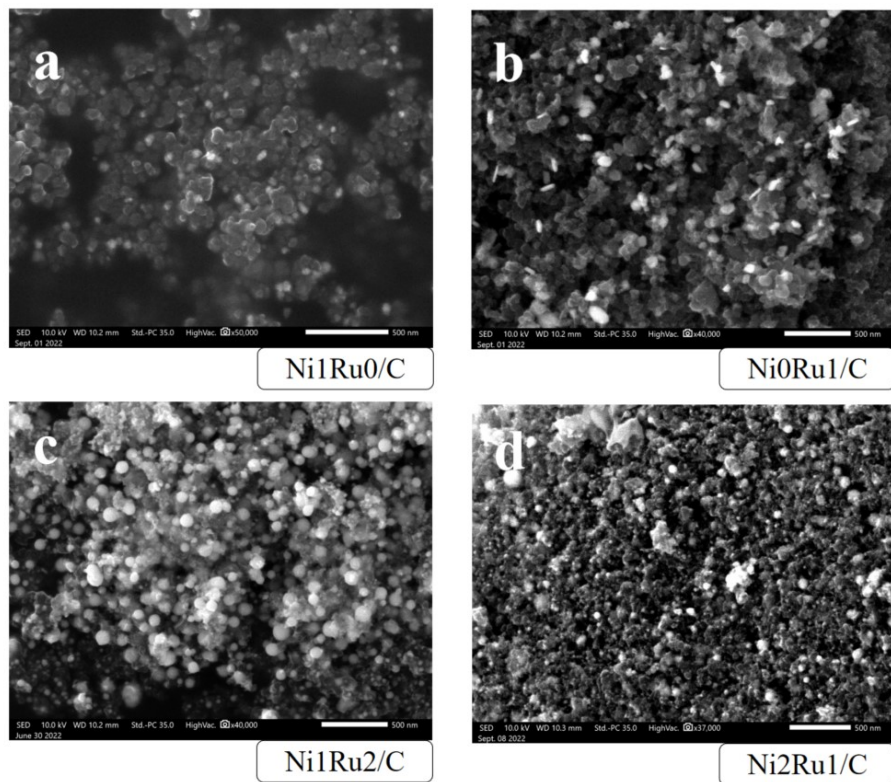

Figure S2. SEM images of (a) Ni1Ru0/C, (b) Ni0Ru1/C, (c) Ni1Ru2/C and

(d) Ni2Ru1/C.
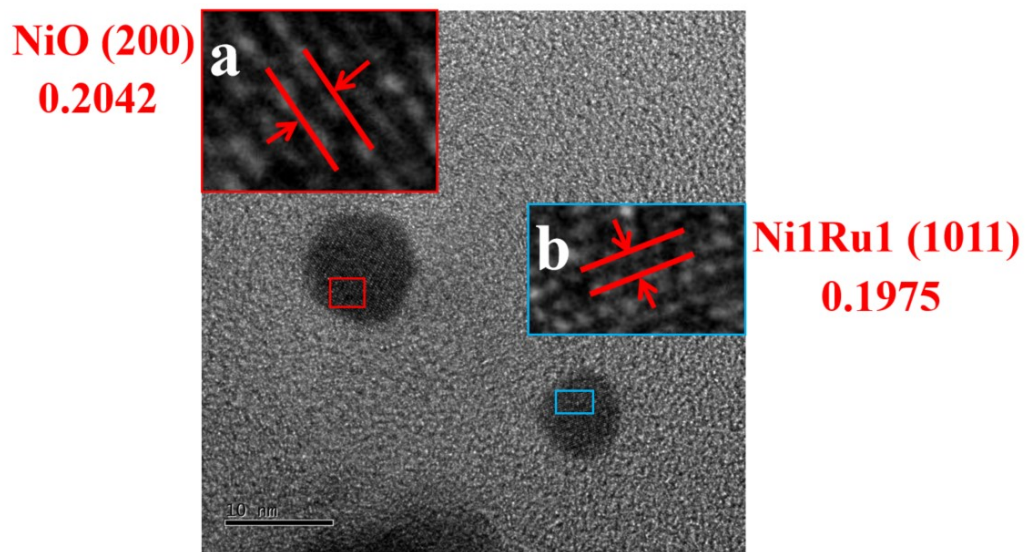
Figure S3. TEM image of Ni1Ru1/C. (a) Large image of the fringe spacings of NiO.

(b) Large image of the fringe spacings of Ni1Ru1.
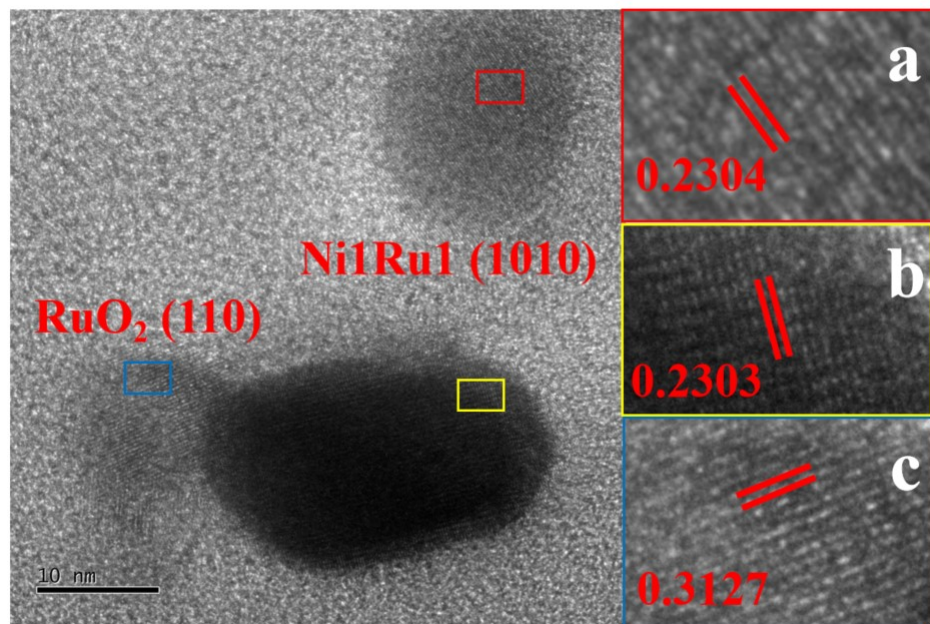
**Figure S4.** TEM image of Ni1Ru1/C. (a), (b) Large image of the fringe spacings of

Ni1Ru1. (c) Large image of the fringe spacings of RuO_2.
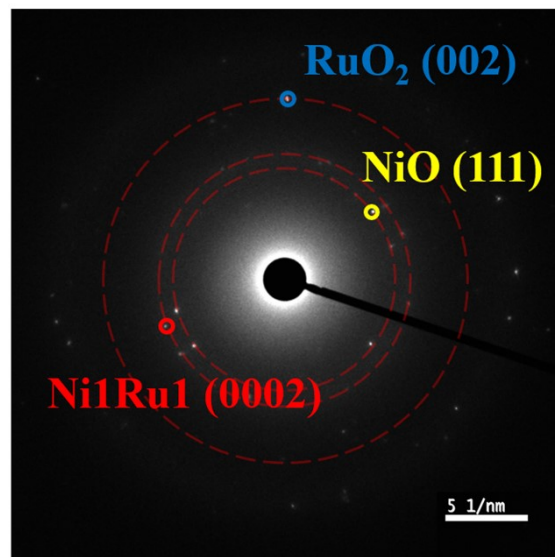
Figure S5. SAED image of Ni1Ru1/C.
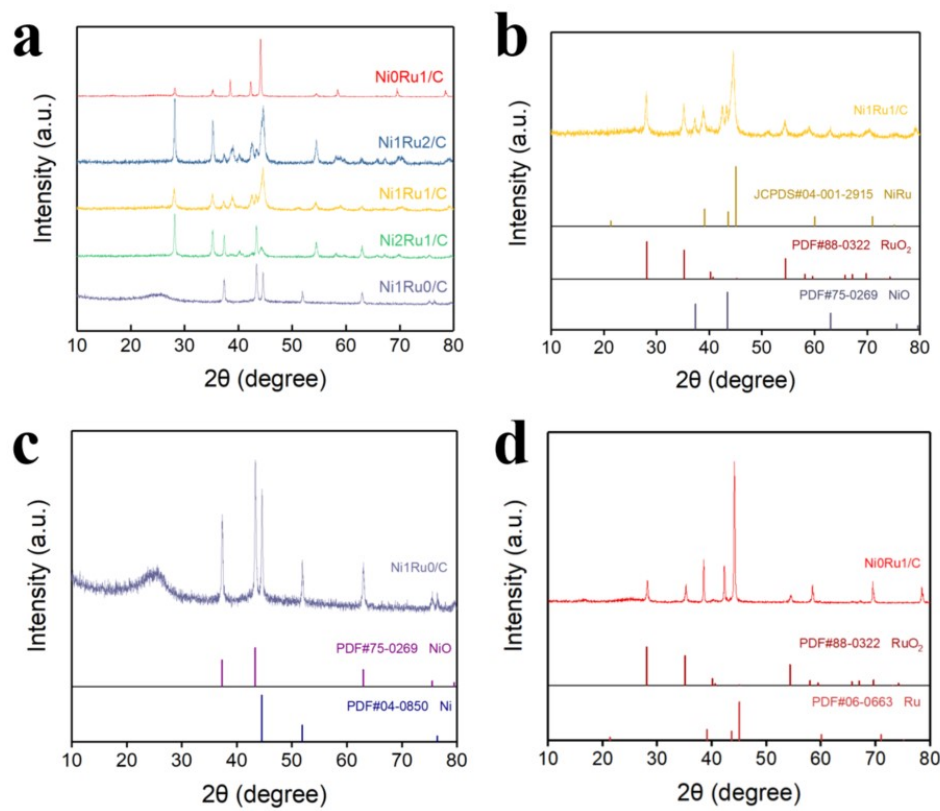
Figure S6. (a) XRD pattern of NixRuy/C. (b) XRD pattern and corresponding PDF cards of Ni1Ru1/C. (c) XRD pattern and corresponding PDF cards of Ni1Ru0/C. (d) XRD pattern and corresponding PDF cards of Ni0Ru1/C.

In addition, Ni1Ru0/C was mainly composed of Ni and NiO and Ni0Ru1/C is mainly

composed of Ru and RuO_2, both of which were multi-component materials.
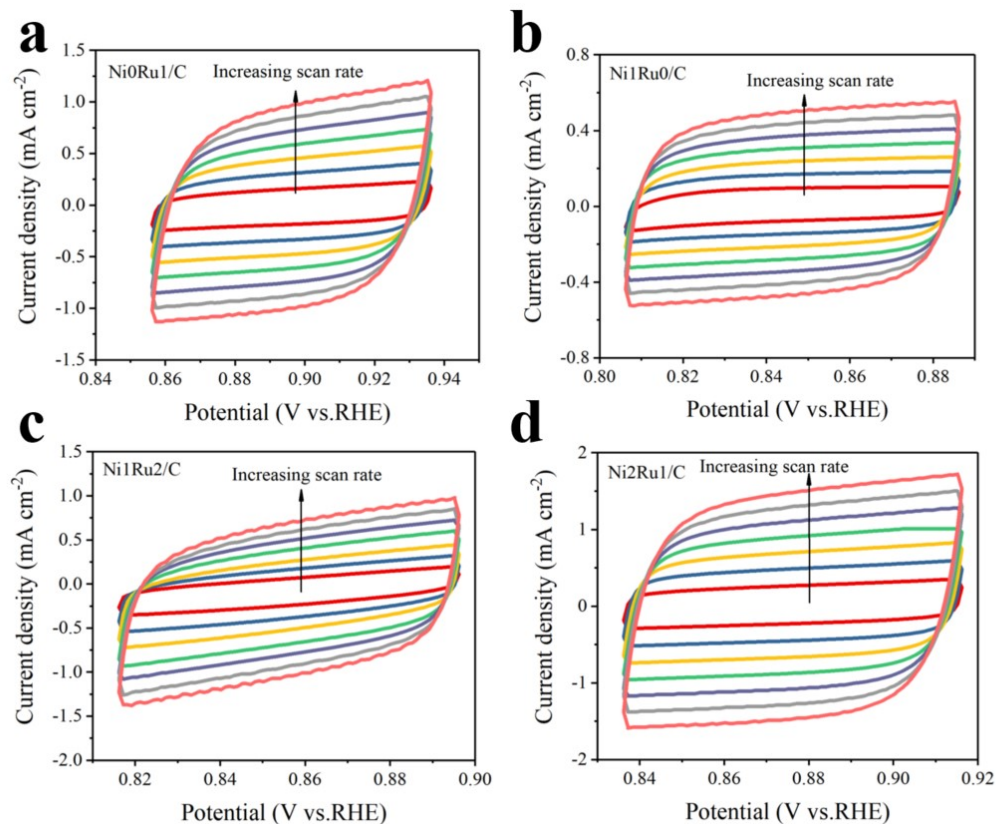
Figure S7. Cyclic voltammograms of (a) Ni1Ru0/C, (b) Ni0Ru1/C, (c) Ni1Ru2/C and

(d) Ni2Ru1/C at scan rates from 10 to 70 mV s^{-1}.
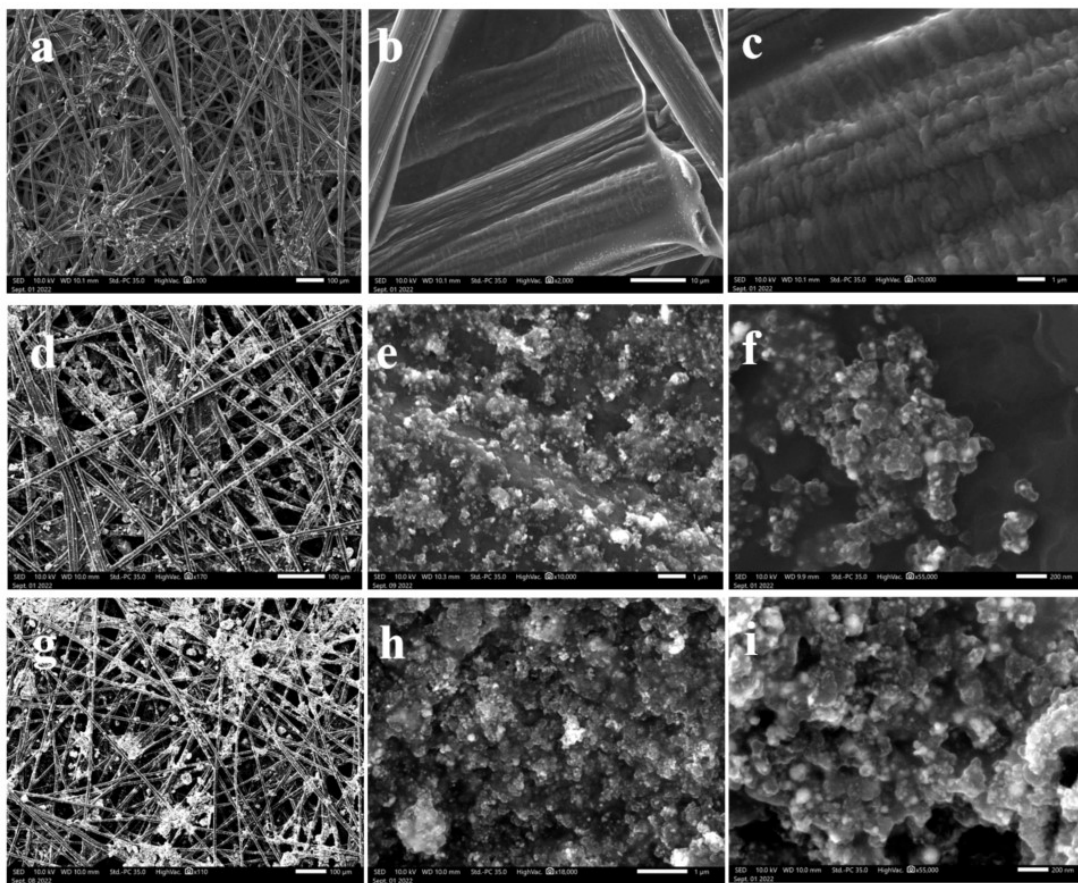
Figure S8. SEM images of (a, b, c) carbon paper, (d, e, f) the electrode of Ni1Ru1/C, and (g, h, i) the electrode of Ni1Ru1/C after 80h of chronoamperometry test.

Compared with (d, e, f) and (g, h, i), it was obvious that the morphology of the electrode surface was not significantly damaged. In detail, there was no obvious aggregation of carbon black on the carbon paper fibers after the test, and the nanoparticles supported on the carbon black basically remained uniformly dispersed.
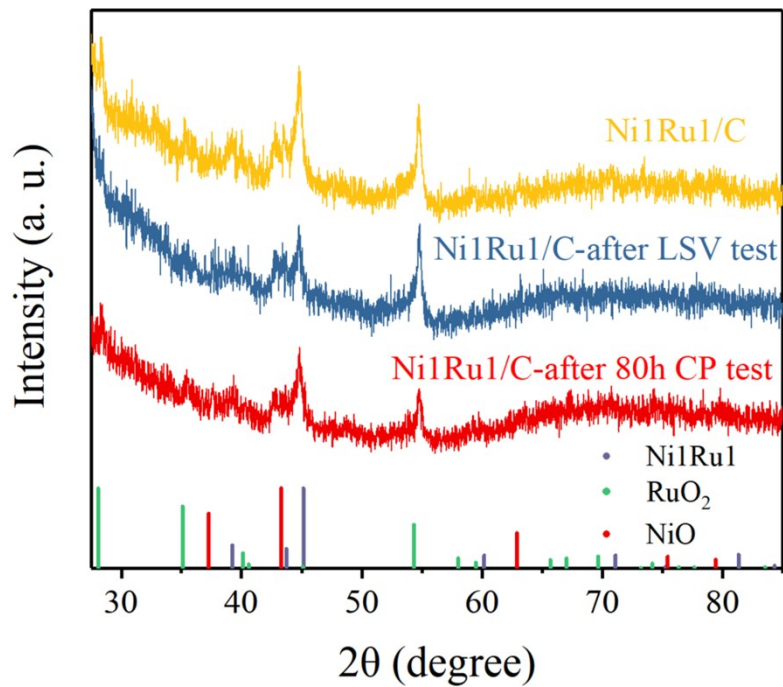
Figure S9. XRD pattern of the electrode of Ni1Ru1/C, Ni1Ru1/C after LSV test, and Ni1Ru1/C after 80h of chronoamperometry test.
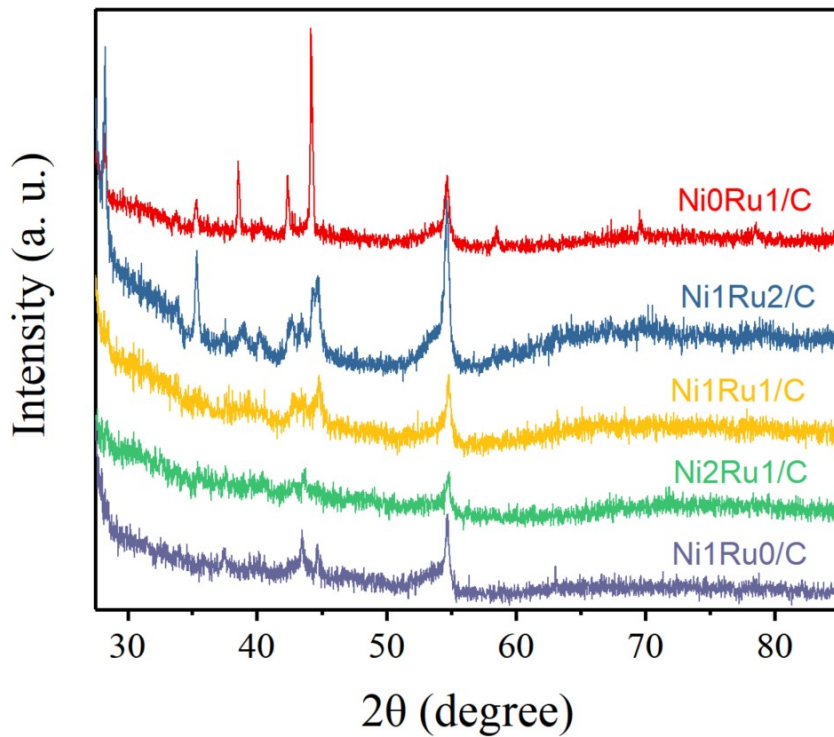
Figure S10. XRD pattern of the electrode of NixRuy/C after LSV test.
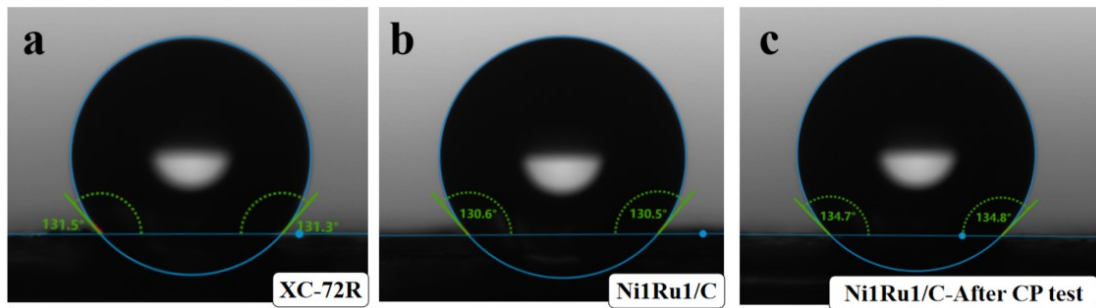
Figure S11. Static water droplets contact angle at the electrode of (a) XC-72R, (b) Ni1Ru1/C, and (c) Ni1Ru1/C after 80h of chronoamperometry test.

Static water droplets contact angle at the electrode of XC-72R, Ni1Ru1/C, and Ni1Ru1/C after 80h of chronoamperometry test was 131.5°, 131.6°, 134.7°, respectively. It was obvious that the electrode of Ni1Ru1/C was hydrophobic and the hydrophobicity was mainly due to the presence of carbon black.
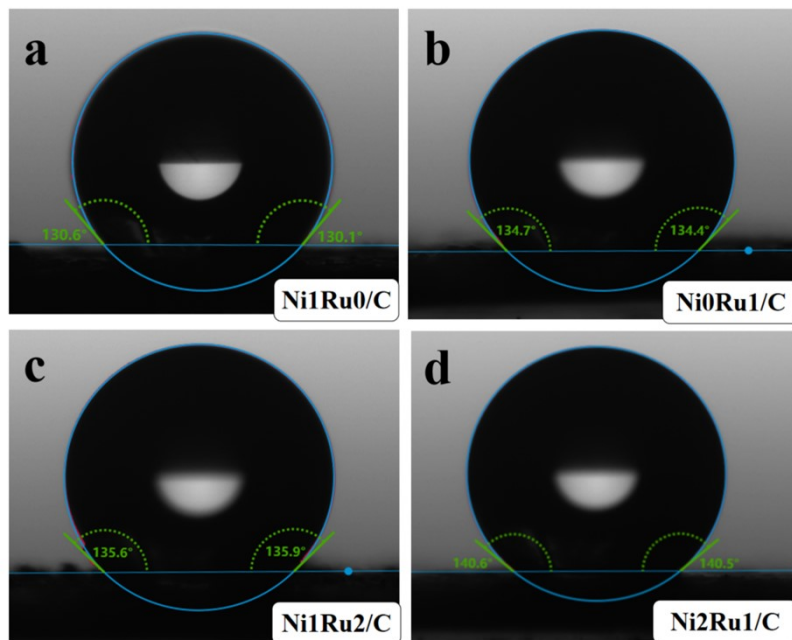
Figure S12. Static water droplets contact angle at electrode of (a) Ni1Ru0/C, (b) Ni0Ru1/C, (c) Ni1Ru2/C and (d) Ni2Ru1/C.

Static water droplets contact angle at the electrode of Ni1Ru0/C, Ni0Ru1/C, Ni1Ru2/C and Ni2Ru1/C was 130.6°, 134.7°, 135.6°, 140.6°, respectively.
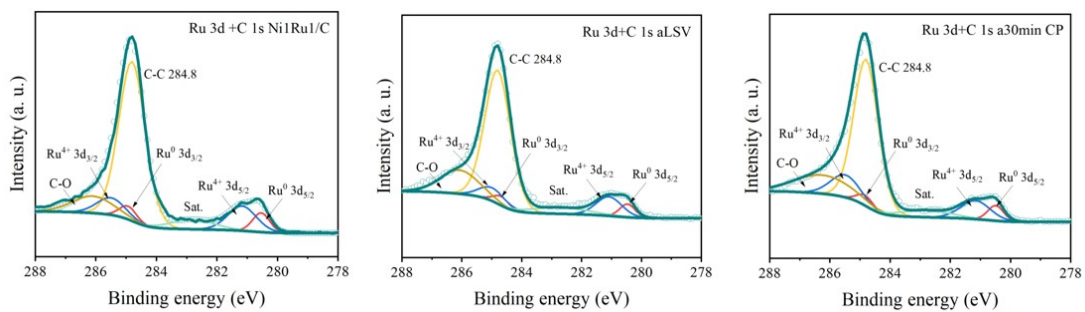
Figure S13. XPS pattern of the electrode of Ni1Ru1/C, Ni1Ru1/C after LSV test, and

Ni1Ru1/C after 30 min of chronoamperometry test at -400 mA cm^{-2}.
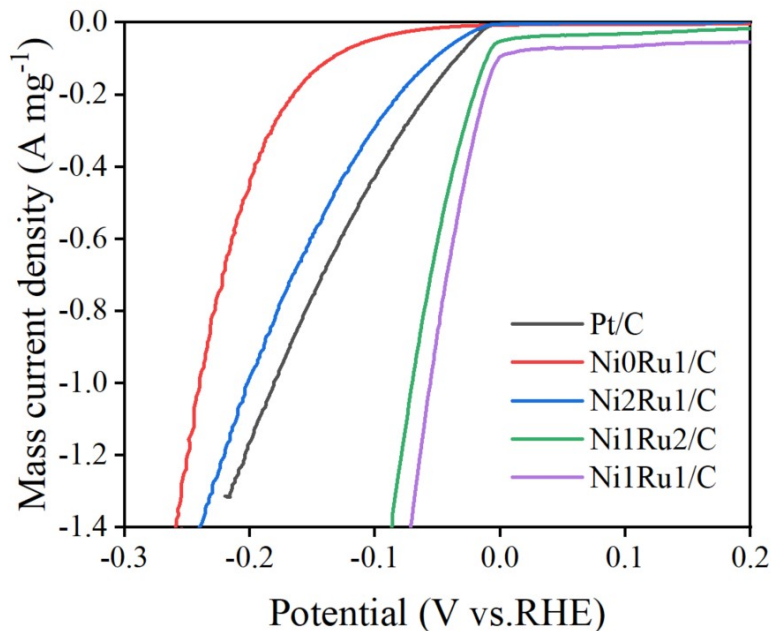
Figure S14 LSV curve obtained by mass current density for NixRuy/C.

Table S1. Comparison of HER activity for NixRuy/C and other reported NiRu electrocatalysts in 1 M KOH.

Electrodes	η_{10} (mV)	η_{100} (mV)	η_{500} (mV)	Tafel slope (mV dec^{-1})	ECSA (mF cm^{-2})	Refs
Ni1Ru1/C	13	46	132	33	23.9	**This work**
Ni2Ru1/C	15	68	171	56	20.2	**This work**
Ni1Ru2/C	16	62	156	44	11.8	**This work**
Cu@NiRu	22	-	-	29.6	32.7	[3]
NiRu/Ni(OH)2	18	142	-	43.3	-	[4]
Ni2P-Ru2P	22	-	-	57	-	[5]
NiRu@NC	19	37	-	37	13.9	[6]
Ru/MXene	37	113	219	60	29	[7]
Ru/RuO2-MoO2	18	201	-	50	58.9	[8]
RuNi1Co1@CMT	78	-	-	77	56.9	[9]
Ni–Ru–P	57	-	-	27.8	7.05	[10]
Ni-	32	110	-	54	0.715	[11]
e-Ni0.6Ru0.4@C	33	83	-	30	26.2	[12]
NiRu-MOF/NF	-	156	-	90	1.77	[13]
R-NiRu	16	-	-	40	58	[14]
NiRu@MWCNTs	14	-	-	32	-	[15]
Pt/NiRu-OH	38	-	-	39	-	[16]
NiRu2@NC-600	53			38	7.28	[17]
Ni@Ru/CNS-10%	20.1			87.3	0.05	[18]
S-2(NiRu@N–C)	32			64	-	[19]

Table S2. Summary of the adding amounts of the precursors for the preparation of various NixRuy/C samples.

Samples	Adding amount of Ni(acac)$_2$ (mg)	Adding amount of RuCl$_3$·3H$_2$O (mg)	Adding amount of Carbon Black (mg)
Ni0Ru1/C	-	522.94	500.0
Ni1Ru2/C	256.9	522.94	500.0
Ni1Ru1/C	512.3	522.94	500.0
Ni2Ru1/C	512.3	261.47	500.0
Ni1Ru0/C	512.3	-	500.0

Table S3. Details of main reagents and instruments.

Reagent/Instruments	Manufacturer	Purity/Type
Ni(acac)$_2$	Adamas	98%
RuCl$_3$·3H$_2$O	Adamas	98%+
Carbon black	Cabot	XC-72R
Carbon paper	Toray	TGP-H-060
Nafion	Dupont	D520 (5% wt)
Ethylene glycol	SCRC	AR
KOH	Macklin	GR, 95%

Table S4. Details of DFT calculation models and results.

Computational model	Schematic diagram	ΔG_{H*} (eV)	Adsorption site
NiRu-H-1		-0.422	Ni-Ru bridge
NiRu-H-2		-0.473	Ru-Ru bridge
RuO_2/NiRu-1		-0.407	Ru
RuO_2/NiRu-2		-0.240	Ni-Ru bridge
RuO_2/NiRu-3		-0.314	Ni-Ru bridge
Ru/NiRu-1		-0.483	Ni-Ru bridge
Ru/NiRu-2		-0.510	Ru-Ru bridge
Ru/NiRu-3		0.654	Ni-Ru bridge
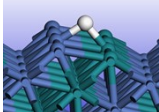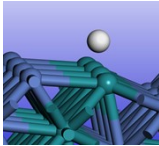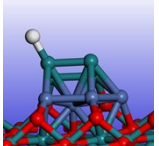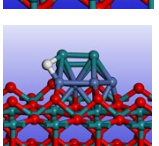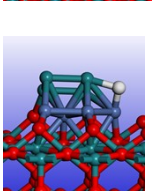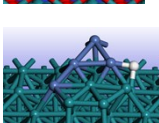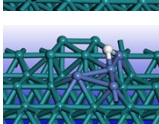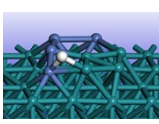
Table S5. Details of area ratio of Ru^{4+} to Ru^0 in XPS pattern (Figure S13).

sample	Area ratio (Ru^{4+} to Ru^0)
Ni1Ru1/C	2.125 (17:8)
Ni1Ru1/C after LSV test	2.333(14:6)
Ni1Ru1/C after CP test	2.143(15:7)

Table S6. Details of mass current activity (Figure S14).

sample	Quality for ICP (mg)	*c_{Ru} (ppm)	$m_{noble-metal}$ (% wt)
Ni2Ru1/C	3.58	0.602	3.363
Ni1Ru1/C	3.90	1.286	6.595
Ni1Ru2/C	3.60	1.086	6.033
Ni0Ru1/C	3.91	0.731	3.739
Pt/C	-	-	40.00

(*) Tested by ICP-OES. Before ICP-OES test, all the samples were dissolved in aqua regia at 150 °C for 24 h (Science Bulletin 67 (2022) 2103–2111), and then diluted to 200 mL with DI.

The mass current density was calculated by the equation below:

$$J_{mass\ current\ density} = \frac{J_{apperent\ current\ density}}{m_{catalyst} \times m_{moble\ metal}\%}$$

(Eq S1.1)

Where $J_{apperent\ current\ density}$ is from the data of Figure 3a, $m_{catalyst}$ is 2 mg (the amount of catalyst taken when preparing the NixRuy/C electrode), $m_{metal}\%$ is obtained from the Table S6.

Table S7. Details of mass current activity (Figure S14).

sample	Current density (A mg^{-1}) at $\eta_{10\ mV}$	Current density (A mg^{-1}) at $\eta_{50\ mV}$	Current density (A mg^{-1}) at $\eta_{100\ mV}$
Ni1Ru1/C	0.17	0.88	2.41
Ni2Ru1/C	0.0075	0.089	0.30
Ni1Ru2/C	0.0091	0.61	1.78
Ni0Ru1/C	0.0075	0.014	0.045
Pt/C	0.012	0.16	0.43

References:

[1] Grimme, S.; Antony, J.; Ehrlich, S.; Krieg, H., A consistent and accurate ab initio parametrization of density functional dispersion correction (DFT-D) for the 94 elements H-Pu. *J Chem Phys* **2010,** *132* (15).

[2] Wang, V.; Xu, N.; Liu, J. C.; Tang, G.; Geng, W. T., VASPKIT: A user-friendly interface facilitating high-throughput computing and analysis using VASP code. *Comput Phys Commun* **2021,** *267*.

[3] Liu, X.; Zhang, S. Y.; Liang, J. S.; Li, S. Z.; Shi, H.; Liu, J. J.; Wang, T. Y.; Han, J. T.; Li, Q., Protrusion-Rich Cu@NiRu Core@shell Nanotubes for Efficient Alkaline Hydrogen Evolution Electrocatalysis. *Small* **2022,** *18* (32).

[4] Zhang, H. Y.; Li, B.; Zou, Y.; Miao, J. H.; Qiao, M.; Tang, Y. J.; Zhang, X.; Zhu, D. D., Acetate promotes the formation of NiRu/NiO towards efficient hydrogen evolution. *Chem Commun* **2022,** *58* (61), 8556-8559.

[5] Yang, D.; Li, P.; Gao, X. Y.; Han, J. L.; Liu, Z. Y.; Yang, Y. P.; Yang, J. H., Modulating surface segregation of Ni2P-Ru2P/CCG nanoparticles for boosting hydrogen evolution reaction in pH-universal. *Chem Eng J* **2022,** *432*.

[6] Jin, W.; Wu, H. B.; Cai, W. Q.; Jia, B. H.; Batmunkh, M.; Wu, Z. X.; Ma, T. Y., Evolution of interfacial coupling interaction of Ni-Ru species for pH-universal water splitting. *Chem Eng J* **2021,** *426*.

[7] Kong, A. Q.; Peng, M.; Gu, H. Z.; Zhao, S. C.; Lv, Y.; Liu, M. H.; Sun, Y. W.; Dai, S. D.; Fu, Y.; Zhang, J. L.; Li, W., Synergetic control of Ru/MXene 3D electrode with superhydrophilicity and superaerophobicity for overall water

splitting. *Chem Eng J* **2021,** *426*.

[8] Fan, Y. X.; Zhang, X. D.; Zhang, Y. J.; Xie, X.; Ding, J.; Cai, J. L.; Li, B. J.; Lv, H. L.; Liu, L. Y.; Zhu, M. M.; Zheng, X. C.; Cai, Q.; Liu, Y. S.; Lu, S. Y., Decoration of Ru/RuO2 hybrid nanoparticles on MoO2 plane as bifunctional electrocatalyst for overall water splitting. *J Colloid Interf Sci* **2021,** *604*, 508-516.

[9] Xue, Y. Q.; Yan, Q.; Bai, X. J.; Xu, Y. Y.; Zhang, X.; Li, Y. J.; Zhu, K.; Ye, K.; Yan, J.; Cao, D. X.; Wang, G. L., Ruthenium-nickel-cobalt alloy nanoparticles embedded in hollow carbon microtubes as a bifunctional mosaic catalyst for overall water splitting. *J Colloid Interf Sci* **2022,** *612*, 710-721.

[10]Wu, K. L.; Sun, K. A.; Liu, S. J.; Cheong, W. C.; Chen, Z.; Zhang, C.; Pan, Y.; Cheng, Y. S.; Zhuang, Z. W.; Wei, X. W.; Wang, Y.; Zheng, L. R.; Zhang, Q. H.; Wang, D. S.; Peng, Q.; Chen, C.; Li, Y. D., Atomically dispersed Ni-Ru-P interface sites for high-efficiency pH-universal electrocatalysis of hydrogen evolution. *Nano Energy* **2021,** *80*.

[11]Gao, T. T.; Li, X. Q.; Chen, X. J.; Zhou, C. X.; Yue, Q.; Yuan, H. Y.; Xiao, D., Ultra-fast preparing carbon nanotube-supported trimetallic Ni, Ru, Fe heterostructures as robust bifunctional electrocatalysts for overall water splitting. *Chem Eng J* **2021,** *424*.

[12]Yang, Q. F.; Jin, P.; Liu, B.; Zhao, L.; Cai, J. H.; Wei, Z.; Zuo, S. W.; Zhang, J.; Feng, L., Ultrafine carbon encapsulated NiRu alloys as bifunctional electrocatalysts for boosting overall water splitting: morphological and electronic modulation through minor Ru alloying. *J Mater Chem A* **2020,** *8* (18), 9049-9057.

[13] Xu, Y.; Yu, S. S.; Ren, T. L.; Liu, S. L.; Wang, Z. Q.; Li, X. N.; Wang, L.; Wang, H. J., Hydrophilic/Aerophobic Hydrogen-Evolving Electrode: NiRu-Based Metal-Organic Framework Nanosheets In Situ Grown on Conductive Substrates. *Acs Appl Mater Inter* **2020,** *12* (31), 34728-34735.

[14] Chen, X. Y.; Wan, J. W.; Wang, J.; Zhang, Q. H.; Gu, L.; Zheng, L. R.; Wang, N.; Yu, R. B., Atomically Dispersed Ruthenium on Nickel Hydroxide Ultrathin Nanoribbons for Highly Efficient Hydrogen Evolution Reaction in Alkaline Media. *Adv Mater* **2021,** *33* (44).

[15] Peng, Z. K.; Liu, J. M.; Hu, B.; Yang, Y. P.; Guo, Y. Q.; Li, B. J.; Li, L.; Zhang, Z. H.; Cui, B. B.; He, L. H.; Du, M., Surface Engineering on Nickel-Ruthenium Nanoalloys Attached Defective Carbon Sites as Superior Bifunctional Electrocatalysts for Overall Water Splitting. *Acs Appl Mater Inter* **2020,** *12* (12), 13842-13851.

[16] Li, D.; Chen, X. F.; Lv, Y. Z.; Zhang, G. Y.; Huang, Y.; Liu, W.; Li, Y.; Chen, R. S.; Nuckolls, C.; Ni, H. W., An effective hybrid electrocatalyst for the alkaline HER: Highly dispersed Pt sites immobilized by a functionalized NiRu-hydroxide. *Appl Catal B-Environ* **2020,** *269*.

[17] Xu, S. K.; Li, Z. Q.; Chu, K. N.; Yao, G.; Xu, Y.; Niu, P.; Zheng, F. C., NiRu nanoparticles encapsulated in a nitrogen-doped carbon matrix as a highly efficient electrocatalyst for the hydrogen evolution reaction. *Dalton T* **2020,** *49* (39), 13647-13654.

[18] Wu, W.; Wu, Y.; Zheng, D.; Wang, K.; Tang, Z. H., Ni@Ru core-shell

nanoparticles on flower-like carbon nanosheets for hydrogen evolution reaction at All-pH values, oxygen evolution reaction and overall water splitting in alkaline solution. *Electrochim Acta* **2019,** *320*.

[19] Xu, Y.; Yin, S. L.; Li, C. J.; Deng, K.; Xue, H. R.; Li, X. N.; Wang, H. J.; Wang, L., Low-ruthenium-content NiRu nanoalloys encapsulated in nitrogen-doped carbon as highly efficient and pH-universal electrocatalysts for the hydrogen evolution reaction. *J Mater Chem A* **2018,** *6* (4), 1376-1381.